Published in final edited form as:
*Biomaterials*. 2013 November ; 34(33): 8213–8222. doi:10.1016/j.biomaterials.2013.07.033.

# The use of surface immobilization of P-selectin glycoprotein ligand-1 on mesenchymal stem cells to facilitate selectin mediated cell tethering and rolling

**Chi Y. Lo**[1], **Aristotelis Antonopoulos**[3], **Anne Dell**[3], **Stuart M. Haslam**[3], **Techung Lee**[4], and **Sriram Neelamegham**[1,2,*]

[1] Department of Chemical and Biological Engineering, The State University of New York, 906 Furnas Hall, Buffalo, NY 14260, USA

[2] The NY State Center for Excellence in Bioinformatics and Life Sciences, The State University of New York, 701 Ellicott St., Buffalo, NY 14203, USA

[3] Department of Life Sciences, Imperial College, South Kensington campus, London SW7 2AZ, UK

[4] Department of Biochemistry, The State University of New York, 140 Farber Hall, Buffalo, NY 14214, USA

## Abstract

Mesenchymal stem/stromal cells (MSCs) are an important candidate for cell-based therapy since they can be easily isolated and expanded, secrete beneficial paracrine factors, and differentiate into multiple lineages. Since the endothelium at sites of injury and inflammation often express adhesion molecules belonging to the selectin family, methods to endow MSCs with selectin-ligands can enhance the efficacy of cell delivery and tissue engraftment. Here, we describe a construct 19Fc[FUT7$^{+}$], where the first 19 amino acids of the pan-selectin ligand PSGL-1 (P-selectin glycoprotein ligand-1) was fused to a human IgG1. When expressed in HEK293T cells over-expressing the α(1,3)fucosyltransferase FUT7, 19Fc[FUT7$^{+}$] is decorated by a core-2 sialyl Lewis-X sialofucosylated O-glycan. The non-covalent coupling of this protein onto MSC surface using palmitated protein G (PPG) enhanced cell binding to E- and P-selectin under hydrodynamic shear, without altering MSC multipotency. MSCs functionalized with 19Fc[FUT7$^{+}$] were captured/tethered onto stimulated endothelial cell monolayers at wall shear stresses up to 4 dyn/cm$^2$. Once captured, the cells rolled robustly up to the highest shear stress tested, 10 dyn/cm$^2$. Unlike previous work where MSCs could only be captured onto selectin-bearing substrates at low or no-flow conditions, the current work presents a ‘glycan engineering’ strategy to enable leukocyte-like capture and rolling.



* Corresponding Author: Department of Chemical and Biological Engineering, and The NY State Center for Excellence in Bioinformatics and Life Sciences, 906 Furnas Hall, State University of New York, Buffalo, NY 14260, USA; Tel.: +1 716 645 1200; Fax: +1 716 645 3822. neel@buffalo.edu (S. Neelamegham).

**Keywords**

mesenchymal stem cells; adhesion molecule; blood flow; cell adhesion; recombinant protein; endothelial cell

## 1. INTRODUCTION

Mesenchymal stem/stromal cell (MSC) therapy has shown great promise in the treatment of many autoimmune disorders and degenerative diseases such as graft-versus-host disease, systemic lupus erythematosus, multiple sclerosis, type 1 diabetes, myocardial infarction, liver cirrhosis and inflammatory bowel disease [1]. For such therapies, MSCs can be scaled-up to produce billions of cells from a single bone marrow aspirate or other connective tissue sources [2]. Once delivered to the target organ, the MSCs repair tissue by acting as a source of paracrine factors that promote cell survival and growth, regulate vascular permeability and promote immune-tolerance [1, 3]. A portion of these multipotent cells may also differentiate and integrate into various host tissue types including bone, adipose, cardiac, cartilage and muscle [2, 4].

The effective use of MSC therapy requires the targeting of cells to the proximity of the tissue repair site with high efficiency. The direct local injection of MSCs into the tissue and the systemic infusion of these cells in blood vessels proximal to the therapeutic site represent two potential delivery routes. While both strategies are viable, systemic infusion has the advantage of being minimally invasive, and it circumvents problems associated with calcification and tissue damage [5, 6]. It can also be applied to target a broad region of the injured tissue that is perfused by blood rather than a local site that may or may not be oxygenated. A shortcoming of this approach, however, is that the efficiency of unmodified MSC captured from flowing blood onto the vascular endothelium is low since selectin-ligands like P-selectin glycoprotein ligand-1 (PSGL-1) are not expressed on these cells. The expression levels of other cell adhesion molecules like VLA-4 and the chemokine receptor CXCR4 on MSCs are also low (<10%) compared to primary leukocytes [7, 8], and can be heterogeneous depending on the MSC isolation protocol and cell culture conditions [4, 6]. Due to this, unmodified MSCs only interact with P- and E-selectin bearing substrates at low wall shear stresses < 0.5 dyn/cm$^2$, and the cell interaction is weak with rolling velocities that are ~50% of the estimated free stream velocity [7, 8]. Thus, a low frequency of MSC capture results, with < 2% of the infused cells being localized at the site of therapy [9, 10]. Because of the low capture frequency, the number of MSCs administered during systemic delivery is large with 0.4-10 million cells per kg bodyweight being introduced per infusion in human clinical trials [11, 12]. Such large infusions can diminish the benefits of MSC therapy since this can contribute to passive MSC entrapment either distal to the infusion site or in other organs like the lung and kidney [10, 13-15].

A variety of surface modification approaches have been undertaken in order to enhance the cell adhesion properties of MSCs since this can improve cell targeting. These methods employ viral transduction to over-express CXCR4 [16], glycan engineering to enhance cellular sialyl Lewis-X (sLe$^X$) content [17], covalent coupling to conjugate sLe$^X$ [18, 19] or E-selectin binding peptides [20] on the cell surface, or non-covalent lipid based methods to couple antibodies against vascular adhesion molecules ICAM-1, VCAM-1 and MAdCAM-1 [21, 22]. In addition to *ex vivo* testing, some of these studies report success in enhancing MSC homing *in vivo* following systemic infusion [16, 17, 22, 23]. Despite these outcomes, strategies to further enhance the efficiency of MSC capture from flowing blood are necessary in order to reduce the number of MSCs applied during therapeutic interventions.

Whereas the previous studies demonstrate that modified MSCs bound under static or low shear stress conditions can continue to adhere upon increasing wall shear stress, they do not demonstrate the direct efficient 'capture' or 'tethering' of MSCs from flow. This is because the molecular binding constants (on-rate, off-rate and $K_D$) for endothelial cell adhesion molecule binding to peptides, antibodies or portions of the natural selectin-ligand (i.e. $sLe^X$ alone) are not suitable for direct cell capture under flow conditions [24]. We overcome this limitation, here, by developing a non-covalent and non-viral strategy to functionalize MSCs with a pan-selectin ligand expressed natively on functional PSGL-1. This ligand, called 19Fc[FUT7$^+$], consists of the first 19 amino acids of PSGL-1 fused to a human IgG tail [25, 26]. A core-2 sialyl Lewis-X glycan is engineered at the N-terminus of this fusion protein in order to confer 'leukocyte-like' cell tethering and rolling properties to MSCs on substrates bearing P- and E-selectin under fluid shear conditions [27]. When immobilized onto MSCs using the palmitated protein G chemistry described earlier [28], this strategy enables MSCs to tether and roll on endothelial cells similar to leukocytes.

## 2. MATERIALS AND METHODS

### 2.1. Antibodies

Mouse anti-human IgG monoclonal antibodies (mAbs) used in this study include anti-PSGL-1/CD162 clone KPL1 (BD Pharmingen, San Jose, CA), anti-P-selectin/CD62P clone G1 (Ancell, Bayport, MN) and anti-E-selectin/CD62E clone CL2/6 (AbD Serotec, Raleigh, NC). Secondary Abs were from either Jackson ImmunoResearch (West Grove, PA) or Invitrogen (Grand Island, NY).

### 2.2. Cell culture

HEK293T cells (HEK, ATCC, Manassas, VA) and P-selectin bearing CHO-P cells available from a previous study were cultured in DMEM (Dulbecco's modified Eagle's medium) supplemented with 10% FBS [29]. Porcine MSCs were cultured in DMEM/F-12 (Cellgro, Manassas, VA) supplemented with 10% FBS and antimycotic (Invitrogen, Grand Island, NY) [14]. These cells were immortalized by cyclin-dependent kinase–1 (CDK1) reprogramming (US patent #20130058903). Human umbilical vein endothelial cells (HUVEC, Lonza, Allendale, NJ) were cultured in supplemented EGM-2 media (Lonza).

### 2.3. Expression, purification and characterization of 19Fc[FUT7$^+$]

Stable HEK cells expressing the α(1,3)fucosyltransferase FUT7 fused to a red fluorescence protein variant (FUT7-DsRED) were generated. To this end, DsRED (after deleting the start codon) was PCR amplified from mRFP-Ubiquitin (Plasmid 11935, Addgene, Cambridge, MA) and this was ligated into the pCS-CG lentiviral vector in place of the green fluorescence protein (Plasmid 12154, Addgene). Human FUT7 available from a previous study [30] was then amplified and ligated upstream of DsRED to make pCS-CG-FUT7-DsRED. Lentiviral particles for FUT7-DsRED were prepared as previously described [30] and these were transduced into HEK cells to create the stable HEK[FUT7$^+$] cell line.

Standard molecular biology methods were used to construct, 19Fc [25]. This fusion protein consists of the first 19 amino acids of PSGL-1 following by an enterokinase cleavage site, a human IgG1 Fc tail, and a 6× His tag. This protein was expressed using the cytomegalovirus (CMV) promoter and von Willebrand Factor signal peptide (VWFsp) in both wild-type HEK and HEK[FUT7$^+$] cell lines. The fusion protein resulting from these two cell types are called '19Fc' and '19Fc[FUT7$^+$]' respectively. The final sequence of the mature 19Fc/19Fc[FUT7$^+$] was verified using Edman degradation of N-terminus and liquid chromatography-mass spectrometry based proteomic sequencing. This sequence is provided in Supplemental Fig. S1.

HEK cells secreting 19Fc and 19Fc[FUT7$^+$] were scaled up in 20 T-150 tissue culture flasks to 80-90% confluency. Cell culture media was then changed to serum-free Pro293a (Lonza). After 3 days 600 mL cell culture supernatant was centrifuged to remove residual cells, filtered via a 0.2 μm membrane filter, and passed through a HisTrap HP column (GE Healthcare, Piscataway, NJ). Following a wash using 20 mM sodium phosphate buffer containing 500 mM NaCl and 50 mM imidazole, the protein was eluted by raising imidazole to 200 mM in the same buffer. 5-10 mg of 19Fc was produced using this procedure.

Purified protein heated to 95°C in the absence (non-reducing condition) or presence (reducing condition) of 0.7 M β-mercaptoethanol was resolved using 4-20% gradient SDS-PAGE. In some cases, these gels were silver stained using a kit from Thermo-Pierce (Rockford, IL). In other cases, the protein was transferred onto a nitrocellulose membrane for western blot analysis using anti-PSGL-1 mAb KPL1 and goat anti-human IgG for detection.

### 2.4. Matrix-assisted laser desorption/ionization-mass spectrometry (MALDI-MS)

19Fc and 19Fc[FUT7$^+$] were treated as described previously [31]. Briefly all samples were subjected to reduction in 4 M guanidine HCl (Thermo-Pierce) containing 2 mg/ml dithiothreitol, carboxymethylation, and trypsin digestion, and the digested glycoproteins were purified by $C_{18}$-Sep-Pak (Waters Corp., Hertfordshire, UK). N-linked glycans were released by peptide:N-glycosidase F (EC 3.5.1.52, Roche Applied Science) digestion, whereas O-linked glycans were released by reductive elimination. N- and O-glycans were then permethylated using the sodium hydroxide procedure, and finally, the permethylated N- and O-glycans were purified by $C_{18}$-Sep-Pak.

All permethylated samples were dissolved in 10 μl of methanol, and 1 μl of dissolved sample was premixed with 1 μl of matrix (for MS, 20 mg/ml 2,5-dihydroxybenzoic acid in 70% (v/v) aqueous methanol; for MS/MS, 20 mg/ml 3,4-diaminobenzophenone in 75% (v/v) aqueous acetonitrile). The mixture was then spotted onto a target plate (2 × 0.5 μl), and dried under vacuum. MS data were acquired using a Voyager-DE STR MALDI-TOF (Applied Biosystems, Darmstadt, Germany). MS/MS data were acquired using a 4800 MALDI-TOF/TOF (Applied Biosystems) mass spectrometer. The collision energy was set to 1 kV, and argon was used as the collision gas. The 4700 calibration standard kit, Calmix (Applied Biosystems), was used as the external calibrant for the MS mode of both instruments, and [Glu1] fibrinopeptide B human (Sigma, St. Louis, MO) was used as an external calibrant for the MS/MS mode of the MALDI-TOF/TOF instrument.

The MS and MS/MS data were processed using Data Explorer 4.9 Software (Applied Biosystems). The spectra were subjected to manual assignment and annotation with the aid of the glycobioinformatics tool, GlycoWorkBench [32]. The proposed assignments for the selected peaks were based on $^{12}C$ isotopic composition together with knowledge of the biosynthetic pathways. The proposed structures were then confirmed by data obtained from MS/MS experiments.

### 2.5. Immobilization of 19Fc and 19Fc[FUT7$^+$] on HEK and MSC surface

Recombinant protein G and palmitic acid N-hydroxysuccinimide ester (NHS-palmitate) (both from Sigma) were coupled [28]. To this end, 0.1 mg/ml NHS-palmitate and 1 mg/ml protein G were incubated at 37°C for 20 h in PBS (pH 7.8) with 0.3% sodium deoxycholate, 0.1% sodium bicarbonate, and 0.1% sodium azide. The resulting palmitated-protein G conjugate or PPG, was then purified using a PD-10 desalting column (GE Healthcare, Piscataway, NJ) using PBS (pH 7.8) with 0.1% sodium deoxycholate as the elution buffer. The product was passed through a 0.45 m cut-off membrane filter. Protein concentration was

determined using a Coomassie Protein Assay Kit (Thermo-Pierce). The buffer was exchanged to PBS just prior to use.

HEK or MSC cells were trypsinized, washed twice and resuspended at $10^7$/mL with HEPES buffer (30 mM HEPES, 110 mM NaCl, 10 mM glucose, 10 mM KCl, 1 mM $MgCl_2$, pH = 7.2). PPG was added to cells at 50-100 μg/ml and the mixture was incubated at 37°C for 1 h with mild agitation. Cells were then washed twice with HEPES buffer prior to addition of 50-100 μg/ml purified 19Fc/19Fc[FUT7$^+$] or Alexa 488 conjugated goat anti-mouse Ab for 30 min at RT. The cells were then washed again in HEPES buffer prior to further experimentation.

### 2.6. Flow cytometry

$2\times10^6$/mL cells in HEPES buffer were incubated with 5-10 μg/ml Ab at RT for 20 minutes. Samples were washed prior to analysis using a FACSCalibur flow cytometer (BD Biosciences).

### 2.7. Alkaline phosphatase assay

Cell viability was determined as necessary using a hemocytometer and the trypan blue exclusion test. The alkaline phosphate assay was either performed at day 0 using $4\times10^5$ cells, or on days 1, 4 and 7 using cells removed from 6 well plates initially seeded with $2.5\times10^5$, $2\times10^5$ and $1.5\times10^5$ cells, respectively. For the latter time points, cells were removed with 0.25% trypsin/EDTA, and washed twice with HEPES buffer. 0.1% Triton-X in PBS was added to the cell pellet and the samples were crushed with a tissue grinder before centrifuging at 14,000×g for 20 min. The supernatant was removed and samples were normalized to equal protein concentrations. 20 μl of the normalized sample was added to 100 μl ALP (alkaline phosphatase) assay solution containing p-nitrophenol phosphate (Biomedical Research Service Center, Buffalo, NY) for 60 min at 37°C. Absorbance at 414 nm was measured using a Synergy 4 plate reader (BioTek, Winooski, VT).

### 2.8. Confocal Microscopy

Cells were removed from culture dishes with trypsin before incubation with PPG and 19Fc[FUT7$^+$] described above. Next, the cells were washed and incubated with 30 μg/ml FITC conjugated goat anti-human IgG Ab (H+L) [$F(ab')_2$] for 20 min at RT, washed twice using HEPES buffer, fixed using HEPES containing 0.5% paraformaldehyde, pelleted, resuspended with ProLong Gold (Invitrogen) and mounted on microscope slides. Samples were imaged using a Zeiss LSM 710 AxioObserver confocal microscope (Jena, Germany) with a Plan-Apochromat 63x/1.40 Oil DIC objective. All images were acquired under identical exposure conditions.

### 2.9. 19Fc/19Fc[FUT7$^+$] binding to platelets under shear

Blood was drawn from healthy human volunteers into 1:9 sodium citrate following human subject protocols approved by the University at Buffalo Institutional Review Board. Platelet rich plasma (PRP) was obtained by centrifugation of blood at 150 g for 12 min. Platelets in PRP were labeled using 0.5 nM BCECF (2'-7'-bis(carboxyethyl)-5(6)-carboxyfluorescein, Invitrogen). HEK/MSCs were stained with 2.7 μg/ml nuclear stain LDS-751 (Invitrogen) at 37°C. Following platelet activation using 18.8 μM TRAP-6 (thrombin receptor agonist peptide) for 5 min, $10^7$ activated platelets/mL in HEPES buffer containing 1.5 mM $CaCl_2$ and 0.1% human serum albumin (abbreviated HEPES-$Ca^{2+}$) were mixed with $2\times10^6$/mL HEK/MSCs using a VT550 cone-plate viscometer (Thermo-Haake, Newington, NH) [33]. The applied shear rate was 650/s. 10 μL of sample collected at indicated times was diluted into 150 μL HEPES-$Ca^{2+}$ buffer and read immediately using the FACSCalibur flow

cytometer. In some runs, platelet-cell adhesion was blocked by incubation of HEK/MSCs with 10 μg/ml anti-PSGL-1 mAb KPL1 for 10 min. Unless otherwise indicated, all steps were conducted at room temperature.

### 2.10. Cell adhesion to selectin-bearing substrates

CHO-P and HUVECs were plated for 1-2 days on 100 $mm^2$ tissue culture dishes, and allowed to grow to confluence. HUVEC cells were stimulated for 4 h with 17 U/ml human IL-1β (R&D Systems, Minneapolis, MN). The plates are washed once with PBS, a custom 1 cm long × 400 μm wide × 100 μm tall parallel-plate microfluidic flow chamber made of polydimethylsiloxane (PDMS) was vacuum sealed on the selectin-bearing cells, and then the entire assembly was mounted on the stage of a Zeiss AxioObserver microscope (Thornwood, NY). 2-5×$10^6$ HEK or MSCs/mL suspended in HEPES-$Ca^{2+}$ buffer were then perfused over the selectin-bearing substrate at various wall shear stresses. Cell interactions were recorded using a Hamamatsu 1394 ORCA camera (Bridgewater, NJ). Analysis was performed by manually counting the cells at 2:30 min after the start of flow using NIH-ImageJ software. Interacting cells were defined as the sum of the total number of rolling and adherent cells. Rolling velocity was calculated between 2:30-3:00 min by following the trajectory of individual cells. To confirm binding specificity, in some runs, 10 μg/ml anti-CD62P or anti-CD62E blocking mAbs were injected into the flow chamber for 10 min prior to the run. In other runs, 10 μg/ml anti-PSGL-1 mAb KPL1 was incubated with HEK/MSC cells for 10 min prior to cell perfusion into the flow chamber.

For studies that quantified cell retention over a range of wall shear stresses, MSCs bearing 19Fc[$FUT7^+$] were initially allowed to bind to stimulated HUVEC monolayers for 10 min under static conditions. The wall shear stress was then progressively step increased to 0.5, 1.5, 3, 5 and 10 dyn/$cm^2$ in 3 min intervals. In each interval, the density of interacting cells was measured 2:30 min after the initiation of that particular wall shear stress.

### 2.11. Statistics

Student's t-test was performed for dual comparisons. One-way ANOVA followed by the Tukey-Kramer test was used for multiple comparisons. *P*-values < 0.05 were considered significant.

## 3. RESULTS

### 3.1. Expression of core-2 sialyl Lewis-X on 19Fc[$FUT7^+$]

HEK[$FUT7^+$] cells were generated by transducing wild-type HEK cells with lentivirus expressing FUT7-DsRED (**Figure 1**, Supplemental Fig. S2). 19Fc and 19Fc[$FUT7^+$] were expressed in wild-type HEK and HEK[$FUT7^+$] cells respectively (Fig. 1A). Proteins secreted into cell culture media were purified using Ni-chelate chromatography. Both 19Fc and 19Fc[$FUT7^+$] were dimeric with a molecular mass of ~68 KDa. The proteins were obtained at > 95% purity as determined using silver staining of SDS-PAGE gels (Fig. 1B). Their identity was confirmed by performing western blot analysis, using anti-PSGL-1 and anti-human IgG antibodies for detection (Fig. 1B).

N-glycans released using PNGaseF and O-glycans released by reductive β-elimination were permethylated and analyzed using ultra-high sensitivity MALDI-TOF mass spectrometry (Fig. 1C-F). Additional MS/MS analysis was performed as necessary to aid peak assignment. As seen, the relative abundance of O-glycans on 19Fc was different from that on 19Fc[$FUT7^+$] especially with respect to the percentage of α(1,3)fucosylated structures. In this regard, the production of the fusion protein in HEK[$FUT7^+$] cells resulted in a dramatic decrease in the relative abundance of mono- (*m/z* = 1344) and di- (*m/z* = 1706) sialylated

non-fucosylated O-glycans and a corresponding increase in core-2 O-glycans bearing the $sLe^X$ epitope at *m/z* = 1519 and 1880. In contrast to the differences noted with O-glycans, the N-glycans of both 19Fc and 19Fc[FUT7$^+$] were very similar. These were primarily composed of three core fucosylated bi-antennary structures at *m/z* = 1836, 2040, and 2244. 19Fc[FUT7$^+$] also expressed some minor higher molecular mass N-glycans including a terminally fucosylated bi-antennary N-glycan at *m/z* = 2780.

### 3.2. Surface immobilization of 19Fc and 19Fc[FUT7$^+$] on HEK cells

In order to develop a streamlined strategy to non-covalently attach 19Fc/19Fc[FUT7$^+$] on heterologous cells via the IgG tail, recombinant protein G was covalently coupled to *N*-hydroxysuccinimide (NHS) functionalized palmitic acid. This resulted in palmitated-protein G (PPG, **Figure 2**). Upon incubation with HEK cells at 37°C for 1 h, PPG intercalated with the cell membrane, thus resulting in HEK-PPG. The extent of PPG incorporation in HEK cells increased linearly with bulk PPG concentration in the range tested, up to 250 μg/mL (Fig. 2B).

Next, the addition of either 50 μg/mL 19Fc or 19Fc[FUT7$^+$] to HEK-PPG cells in physiological buffers at ambient temperature resulted in HEK-PPG-19Fc and HEK-PPG-19Fc[FUT7$^+$] cells. As expected, FITC-conjugated $F(ab)'_2$ fragments of goat anti-human IgG only bound HEK cells that were coupled with 19Fc or 19Fc[FUT7$^+$] (Fig. 2C). Minimal binding of the antibody fragment to HEK-PPG cells was detected in the absence of the fusion protein. In order to determine the fraction of protein-G binding sites that were occupied on the HEK-PPG cells, we assayed the ability of 19Fc and 19Fc[FUT7$^+$] to prevent the binding of FITC conjugated whole IgG antibody which PPG avidly binds (Fig. 2D). In these runs, FITC-conjugated antibody binding to HEK-PPG cells was reduced by 80% in the presence of 19Fc/19Fc[FUT7$^+$]. Thus, a majority of the PPG sites on HEK cells are occupied by the fusion proteins under our experimental conditions. Confocal microscopy studies performed using FITC-conjugated $F(ab')_2$ fragments of goat anti-human IgG (H+L) demonstrate that all the 19Fc[FUT7$^+$] is localized on the membrane of the HEK cells (Fig. 2D and Supplemental Video A).

### 3.3. HEK-PPG-19Fc[FUT7$^+$] binding to selectins under hydrodynamic shear

Studies were performed to determine if the non-covalent coupling strategy outlined in the preceding section is sufficient to support selectin mediated cell adhesion under hydrodynamic shear conditions. Such studies were performed using both a cone and plate viscometer and a microfluidics based parallel-plate flow chamber (**Figure 3**).

In the viscometer studies (Fig. 3A), HEK cells bearing either 19Fc or 19Fc[FUT7$^+$] were shear mixed with TRAP-6 activated human platelets which express P-selectin on their cell surface. The percentage of HEK cells that bound activated platelets was quantified using flow cytometry. As seen, 40-60% of the HEK cells bearing 19Fc[FUT7$^+$] bound to at least one platelet within 1-3 min of shear application. The binding was specific since it could be blocked by a function blocking anti-PSGL-1 mAb KPL1. HEK cells bearing 19Fc, which lacks the core-2 $sLe^X$, did not bind platelet P-selectin. Wild-type HEK and HEK-PPG cells also did not bind activated platelets. Further, control studies verified that the anti-PSGL-1 mAb used in this study did not inhibit cell adhesion by trivially displacing 19Fc[FUT7$^+$] from the HEK cell surface (Supplemental Fig. S3).

The flow chamber experiments utilized a microfluidic flow cell. Here, various HEK cell types were perfused over substrates composed of either P-selectin bearing CHO-P cells (Fig. 3B) or E-selectin bearing IL-1β stimulated HUVECs (Fig. 3C). At a venular wall shear stress of 1 dyn/cm$^2$, HEK-PPG-19Fc[FUT7$^+$] bound both P- and E-selectin at significantly

higher numbers compared to either the HEK-PPG or HEK-PPG-19Fc cells. Cell-substrate adhesion was blocked by mAbs against the N-terminus of PSGL-1 and also an anti-E-selectin mAb. Thus, the binding of HEK-PPG-19Fc[FUT7$^+$] to P-selectin on platelets and also substrates bearing P-/E-selectin expressing cells is mediated by selectin binding to sialofucosylated glycans on 19Fc[FUT7$^+$].

### 3.4. Effect of 19Fc[FUT7$^+$] immobilization on MSC function

PPG and 19Fc/19Fc[FUT7$^+$] were immobilized onto MSCs using protocols similar to that applied to HEK cells in Fig. 2. Here, the amount of PPG bound to MSCs increased linearly with increasing PPG concentration (Fig. 4A). After 19Fc[FUT7$^+$] was bound to the MSCs, its cell surface concentration decreased gradually to 66% of the original amount at 24 h, and 25% at 72 h (Fig. 4B). Confocal microscopy analysis confirmed the immobilization of 19Fc[FUT7$^+$] on MSC surface (Fig. 4C and Supplemental Video B).

Modification of MSCs with PPG and 19Fc[FUT7$^+$] did not affect cell function. Cell viability measured using trypan blue exclusion remained >98% under all experimental conditions (Fig. 4D), cell proliferation was unaffected (data not shown), and cellular alkaline phosphatase activity was unaltered upon modification (Fig. 4E). Thus, cell modification did not affect osteogenic differentiation potential. Additional experiments confirmed that the differentiation potential of 19Fc[FUT7$^+$] modified stem cells towards chondrogenic and adipogenic lineages was also no different from that of unmodified cells (data not shown).

### 3.5. Tethering and rolling of 19Fc[FUT7$^+$] bearing MSCs on P- and E-selectin

Microfluidics based parallel-plate flow chamber studies evaluated the rolling phenotype of the modified MSCs. Here, the robust interaction of the MSC-PPG-19Fc[FUT7$^+$] cells was observed on P- (Fig. 5A) and E- (Fig. 5B) selectin bearing substrates. A majority of cells tethered and rolled on these substrates as would be expected for cell adhesion mediated by selectin-carbohydrate binding interactions (Supplemental Video C). The MSC-PPG-19Fc[FUT7$^+$] rolling velocity was ~3 μm/s on P-selectin at 1 dyn/cm$^2$, and 11.5 μm/s on E-selectin at 2 dyn/cm$^2$ (Fig. 5C). Neither the coupling of MSC-PPG cells with mAbs against the lectin domain of P-selectin (clone G1, Fig. 5A) nor E-selectin (clone CL2/6, Fig. 5B) resulted in cell capture to selectin bearing substrates under shear. Such studies were performed when the concentration of antibody added to MSC-PPG cells was either identical or double that of 19Fc[FUT7$^+$] bearing cells. Additional controls verified that the selectin-mediated cell adhesion was specific since unmodified MSCs, MSC-PPG and MSC-PPG-19Fc did not bind P-/E-selectin under shear. In addition, MSC-PPG-19Fc[FUT7$^+$] cell adhesion was specifically blocked by blocking mAbs against either the N-terminus of PSGL-1 (clone KPL1) or the lectin domains of P-selectin (clone G1) and E-selectin (clone CL2/6).

Since stimulated endothelial cells represents a physiological cell types that homing MSCs may encounter in the human vasculature, more detailed investigations evaluated: i) the rate of cell capture under hydrodynamic flow over a range of wall shear stresses from 0.5- 4 dyn/cm$^2$ (Fig. 6A, Supplemental Video D), and ii) the retention of previously captured cells upon step increasing wall shear stress (Fig. 6B, Supplemental Video E). In the first study, a significant number of MSC-PPG-19Fc[FUT7$^+$] cells were captured onto IL-1β stimulated HUVECs at shear stresses up to 4 dyn/cm$^2$. In the second study, MSC-PPG-19Fc[FUT7$^+$] cells, once captured under static conditions, were retained on the HUVEC substrate upon increasing the applied shear stress up to the highest shear stress tested (10 dyn/cm$^2$). In control studies, unconjugated MSCs and MSC-PPG cells were neither captured (Fig. 6A) nor retained (Fig. 6B) on the stimulated HUVECs under identical conditions. Overall, the

data demonstrate that the coupling of functional selectin-ligands on MSCs confers leukocyte-like cell adhesion capabilities to this cell type.

# 4. DISCUSSION

## 4.1. Design features of 19Fc[FUT7$^+$]

Cell engineering principles were applied to non-covalently incorporate 19Fc[FUT7$^+$] onto MSCs. The overall experimental approach had three goals. First, we aimed to create a dimeric fusion protein containing the N-terminal selectin-binding epitope of human PSGL-1. In this regard, like PSGL-1, the N-terminus of 19Fc[FUT7$^+$] incorporates an O-linked core-2 sLe$^X$ glycan since this carbohydrate, when presented in the context of the acidic PSGL-1 backbone, binds all three members of the selectin family (L-, E- and P-selectin) under physiologic fluid shear conditions [34]. 19Fc[FUT7$^+$] is also dimeric like native PSGL-1. In addition, by testing a range of promoters and signal peptide sequences in our expression construct, the production of 19Fc[FUT7$^+$] in HEK[FUT7$^+$] cells was optimized (data not shown). Second, we wished to create a natural construct since this would minimize potential immunogenicity during human applications. In this regard, all the O-glycans of 19Fc[FUT7$^+$], as measured using mass spectrometry, have been previously reported to be expressed on human neutrophils [35]. In addition, the N-glycans of 19Fc[FUT7$^+$] are similar to that reported in previous studies that characterize the N-glycans of human IgG1 [36, 37]. These features should contribute to low immunogenicity during human applications. Third, non-covalent and non-viral strategies were applied for temporary and rapid complexing of 19Fc[FUT7$^+$] onto MSCs since this glycoprotein is only required during the initial cell capture step. This simple, non-permanent immobilization method did not alter MSC viability, proliferation or multipotency. 19Fc[FUT7$^+$] immobilized on MSCs plasma membranes decreased gradually to 25% of the original amount over a time period of 3 days. This decrease is most likely related to the regular endocytosis of the cell and maybe partially due to extracellular loss, similar to normal glycoprotein and glycolipid turnover on plasma membranes [38].

## 4.2. Rolling phenotype of 19Fc[FUT7$^+$] functionalized MSCs

Functionalization of MSCs with 19Fc[FUT7$^+$] endowed MSCs with leukocyte-like tethering and rolling properties. These cells could be captured onto E-selectin bearing activated endothelial cells at wall shear stresses up to 4 dyn/cm$^2$. Once captured, robust cell retention was observed at wall shear stress ≥ 10 dyn/cm$^2$. Cell rolling velocity was in the range of 3-12 μm/s on selectin bearing substrates at 1-2 dyn/cm$^2$. These features are reminiscent of human neutrophils rolling on P/E-selectin [39].

In general, 19Fc[FUT7$^+$] mimics the natural ligands of the vascular adhesion molecules more closely compared to previous approaches developed by others [16-21]. In one approach, antibodies against immunoglobulin superfamily receptors (anti-ICAM-1, anti-VCAM-1, and anti-MAdCAM) were coupled onto MSCs in order to enhance their cell adhesion properties [21, 22]. This method required the stoppage of flow to allow MSC binding since the binding constants for protein-antibody binding are not optimum for cell capture under continuous flow. In agreement with this, the current study demonstrates that the coupling of anti P- and E-selectin antibodies to MSCs alone does not enable cell tethering/capture from flow. A second strategy, utilizes viral transduction to express either an erbB2 artificial receptor [40] or CXCR4 [16] on MSCs in order to enhance cell homing properties. Such permanent viral modification strategies may raise safety concerns that are mitigated by the non-covalent coupling approach presented in the current manuscript. A third approach decorates the MSC surface with either sLe$^X$ [18] or E-selectin binding peptides that has been identified using phage display [20]. While sLe$^X$ modified cells rolled

on recombinant P-selectin *in vitro* up to 0.75 dyn/cm$^2$ [18], the *in vivo* rolling velocity of these cells in post-capillary venules was high at ~60% of the velocity of non-interacting cells [19]. Here, functionalization of sLe$^X$ alone may be insufficient to enable stable rolling since, in natural selectin-ligands, this tetrasaccharide is presented in the context of a glycan-core and protein/lipid backbone structure [41]. The peptide conjugation approach also similarly demonstrates tethering onto E-selectin substrates at wall shear stress below 0.25 dyn/cm$^2$ [20], though cell rolling was sustained at shear stresses up to 10 dyn/cm$^2$ after cell capture. One possible explanation for this is that the E-selectin binding peptide conjugate used in this study was originally designed using phage display for the purpose of competitively inhibiting E-selectin binding function and not specifically for capturing cells under shear flow.

While the current study using 19Fc[FUT7$^+$] demonstrates cell capture on endothelial cells up to 2-4 dyn/cm$^2$, this may be further improved by incorporating additional physiological selectin-ligands, particularly those that bind E-selectin efficiently. For example, Sackstein *et al*. [17] demonstrate that the *ex vivo* α(1,3)-fucosylation of MSCs enables E-selectin binding potentially by converting the endogenous CD44 receptor on MSCs into a sialofucosylated form called HCELL (hematopoietic cell E-selectin/L-selectin ligand). These investigators show that the enzymatically modified MSCs captured at low flow conditions (0.5 dyn/cm$^2$) can subsequently sustain rolling interactions up to 30 dyn/cm$^2$. Thus, combining the functionality of HCELL with 19Fc[FUT7$^+$] may enhance both MSC tethering and rolling on activated endothelial substrates. Here, 19Fc[FUT7$^+$] would enable cell tethering to P- and E-selectin, with HCELL enhancing the robustness of E-selectin mediated cell rolling. Such modification with HCELL may also enhance MSC diapedesis/transmigration as discussed below.

### 4.3. Transmigration across the endothelial barrier

In the multistep leukocyte cell adhesion cascade, leukocyte adhesion to the inflamed endothelium is followed by transmigration through the vessel wall. Though the current study does not focus on the mechanism of MSC extravasation from blood and the effect of 19Fc[FUT7$^+$] coupling on this process, others have studied the MSC transmigration step [5, 7, 42]. This diapedesis process has leukocyte-like features, only it occurs in the time scale of 30-120 min, compared to granulocytes which transmigrate within 2-6 min [42]. The initiation of MSC transmigration is preceded by the formation of non-apoptotic membrane blebs which push on and breach the endothelium, much like embryonic and tumor cells [42]. The complete transmigration mechanism has yet to be revealed, though several potential molecular players have been identified: VCAM-1/VLA-4, MMP-2, cytokines and chemokines (CXCL9, CXCL16, CCL20, and CCL25) [5, 43]. In these models, chemokine binding to G-protein-coupled receptors initiates MSC signaling through Gαi thus promoting transmigration. As the MSCs begin to extravasate, protrusions form from the endothelial cells creating transmigratory cups that surround the MSC [42]. Both paracellular (via endothelial cell junctions) and transcellular (directly through endothelial cells) routes are thought to contribute to MSC transmigration [42]. Besides these canonical pathways that are beginning to be documented in native MSCs, the *ex vivo* α(1,3)-fucosylation of MSCs is also thought to trigger additional transmigration mechanisms via E-selectin dependent cell signaling. In the context of the current work, enhancing MSC capture frequency on endothelial cells using 19Fc[FUT7$^+$] may provide greater opportunities for cell transmigration to therapeutic sites.

## 5. CONCLUSIONS

In summary, the ability to home MSCs for tissue repair under continuous flow is important in the context of systemic delivery. The current study demonstrates a simple and robust strategy to achieve this by coupling 19Fc[FUT7$^+$] to the MSC surface. Such functionalization enables leukocyte-like selectin mediated MSC tethering and rolling on stimulated endothelial cells under shear flow.

## Supplementary Material

Refer to Web version on PubMed Central for supplementary material.

## Acknowledgments

This work was supported by an American Heart Pre-doctoral Fellowship (to C.L.), the Biotechnology and Biological Sciences Research Council Grants (to A. D. and S. M. H. for Core Support for Collaborative Research), a New York State Stem Cell Contract C024282 (to S.N.), and NIH grants HL63014 and HL103411 (to S.N.).

## Abbreviation

| | |
|---|---|
| **PPG** | Palmitated-protein G conjugate |
| **19Fc and 19Fc[FUT7$^+$]** | Fusion protein of PSGL-1 N-terminal peptide fused to human IgG1 Fc expressed in either wild-type HEK293T (HEK) or HEK overexpressing α(1,3)fucosyltransferase, FUT7 |

## REFERENCES

1. Ren G, Chen X, Dong F, Li W, Ren X, Zhang Y, et al. Concise review: mesenchymal stem cells and translational medicine: emerging issues. Stem Cells Transl Med. 2012; 1:51–8. [PubMed: 23197640]
2. Pittenger MF, Mackay AM, Beck SC, Jaiswal RK, Douglas R, Mosca JD, et al. Multilineage potential of adult human mesenchymal stem cells. Science. 1999; 284:143–7. [PubMed: 10102814]
3. Uccelli A, Moretta L, Pistoia V. Mesenchymal stem cells in health and disease. Nat Rev Immunol. 2008; 8:726–36. [PubMed: 19172693]
4. Phinney DG, Prockop DJ. Concise review: mesenchymal stem/multipotent stromal cells: the state of transdifferentiation and modes of tissue repair--current views. Stem Cells. 2007; 25:2896–902. [PubMed: 17901396]
5. Steingen C, Brenig F, Baumgartner L, Schmidt J, Schmidt A, Bloch W. Characterization of key mechanisms in transmigration and invasion of mesenchymal stem cells. J Mol Cell Cardiol. 2008; 44:1072–84. [PubMed: 18462748]
6. Karp JM, Leng Teo GS. Mesenchymal stem cell homing: the devil is in the details. Cell Stem Cell. 2009; 4:206–16. [PubMed: 19265660]
7. Ruster B, Gottig S, Ludwig RJ, Bistrian R, Muller S, Seifried E, et al. Mesenchymal stem cells display coordinated rolling and adhesion behavior on endothelial cells. Blood. 2006; 108:3938–44. [PubMed: 16896152]
8. Thankamony SP, Sackstein R. Enforced hematopoietic cell E- and L-selectin ligand (HCELL) expression primes transendothelial migration of human mesenchymal stem cells. Proc Natl Acad Sci USA. 2011; 108:2258–63. [PubMed: 21257905]
9. Barbash IM, Chouraqui P, Baron J, Feinberg MS, Etzion S, Tessone A, et al. Systemic delivery of bone marrow-derived mesenchymal stem cells to the infarcted myocardium: feasibility, cell migration, and body distribution. Circulation. 2003; 108:863–8. [PubMed: 12900340]
10. Devine SM, Cobbs C, Jennings M, Bartholomew A, Hoffman R. Mesenchymal stem cells distribute to a wide range of tissues following systemic infusion into nonhuman primates. Blood. 2003; 101:2999–3001. [PubMed: 12480709]

11. Macmillan ML, Blazar BR, DeFor TE, Wagner JE. Transplantation of ex-vivo culture-expanded parental haploidentical mesenchymal stem cells to promote engraftment in pediatric recipients of unrelated donor umbilical cord blood: results of a phase I-II clinical trial. Bone Marrow Transplant. 2009; 43:447–54. [PubMed: 18955980]
12. Le Blanc K, Frassoni F, Ball L, Locatelli F, Roelofs H, Lewis I, et al. Mesenchymal stem cells for treatment of steroid-resistant, severe, acute graft-versus-host disease: a phase II study. Lancet. 2008; 371:1579–86. [PubMed: 18468541]
13. Freyman T, Polin G, Osman H, Crary J, Lu M, Cheng L, et al. A quantitative, randomized study evaluating three methods of mesenchymal stem cell delivery following myocardial infarction. Eur Heart J. 2006; 27:1114–22. [PubMed: 16510464]
14. Leiker M, Suzuki G, Iyer VS, Canty JM, Lee T. Assessment of a nuclear affinity labeling method for tracking implanted mesenchymal stem cells. Cell Transplantation. 2008; 17:911–22. [PubMed: 19069634]
15. Millard SM, Fisk NM. Mesenchymal stem cells for systemic therapy: shotgun approach or magic bullets? Bioessays. 2013; 35:173–82. [PubMed: 23184477]
16. Cheng Z, Ou L, Zhou X, Li F, Jia X, Zhang Y, et al. Targeted migration of mesenchymal stem cells modified with CXCR4 gene to infarcted myocardium improves cardiac performance. Mol Ther. 2008; 16:571–9. [PubMed: 18253156]
17. Sackstein R, Merzaban JS, Cain DW, Dagia NM, Spencer JA, Lin CP, et al. Ex vivo glycan engineering of CD44 programs human multipotent mesenchymal stromal cell trafficking to bone. Nat Med. 2008; 14:181–7. [PubMed: 18193058]
18. Sarkar D, Vemula PK, Zhao W, Gupta A, Karnik R, Karp JM. Engineered mesenchymal stem cells with self-assembled vesicles for systemic cell targeting. Biomaterials. 2010; 31:5266–74. [PubMed: 20381141]
19. Sarkar D, Spencer JA, Phillips JA, Zhao W, Schafer S, Spelke DP, et al. Engineered cell homing. Blood. 2011; 118:e184–91. [PubMed: 22034631]
20. Cheng H, Byrska-Bishop M, Zhang CT, Kastrup CJ, Hwang NS, Tai AK, et al. Stem cell membrane engineering for cell rolling using peptide conjugation and tuning of cell-selectin interaction kinetics. Biomaterials. 2012; 33:5004–12. [PubMed: 22494889]
21. Ko IK, Kean TJ, Dennis JE. Targeting mesenchymal stem cells to activated endothelial cells. Biomaterials. 2009; 30:3702–10. [PubMed: 19375791]
22. Ko IK, Kim BG, Awadallah A, Mikulan J, Lin P, Letterio JJ, et al. Targeting improves MSC treatment of inflammatory bowel disease. Mol Ther. 2010; 18:1365–72. [PubMed: 20389289]
23. Guan M, Yao W, Liu R, Lam KS, Nolta J, Jia J, et al. Directing mesenchymal stem cells to bone to augment bone formation and increase bone mass. Nat Med. 2012; 18:456–62. [PubMed: 22306732]
24. Beauharnois ME, Lindquist KC, Marathe D, Vanderslice P, Xia J, Matta KL, et al. Affinity and kinetics of sialyl Lewis-X and core-2 based oligosaccharides binding to L- and P-selectin. Biochemistry. 2005; 44:9507–19. [PubMed: 15996105]
25. Lo CY, Antonopoulos A, Gupta R, Qu J, Dell A, Haslam SM, et al. Competition between core-2 GlcNAc-transferase and ST6GalNAc-transferase regulates the synthesis of the leukocyte selectin ligand on human P-selectin glycoprotein ligand-1. J Biol Chem. 2013; 288:13974–87. [PubMed: 23548905]
26. Goetz DJ, Greif DM, Ding H, Camphausen RT, Howes S, Comess KM, et al. Isolated P-selectin glycoprotein ligand-1 dynamic adhesion to P- and E-selectin. J Cell Biol. 1997; 137:509–19. [PubMed: 9128259]
27. Jones DA, Smith CW, McIntire LV. Leucocyte adhesion under flow conditions: principles important in tissue engineering. Biomaterials. 1996; 17:337–47. [PubMed: 8745331]
28. Kim SA, Peacock JS. The use of palmitate-conjugated protein A for coating cells with artificial receptors which facilitate intercellular interactions. J Immunol Methods. 1993; 158:57–65. [PubMed: 8429217]
29. Marathe DD, Buffone A Jr. Chandrasekaran EV, Xue J, Locke RD, Nasirikenari M, et al. Fluorinated per-acetylated GalNAc metabolically alters glycan structures on leukocyte PSGL-1 and reduces cell binding to selectins. Blood. 2010; 115:1303–12. [PubMed: 19996411]

30. Buffone A Jr. Mondal N, Gupta R, McHugh KP, Lau JT, Neelamegham S. Silencing alpha 1,3-fucosyltransferases in human leukocytes reveals a role for FUT9 enzyme during E-selectin-mediated cell adhesion. J Biol Chem. 2013; 288:1620–33. [PubMed: 23192350]

31. Jang-Lee J, North SJ, Sutton-Smith M, Goldberg D, Panico M, Morris H, et al. Glycomic profiling of cells and tissues by mass spectrometry: fingerprinting and sequencing methodologies. Methods Enzymol. 2006; 415:59–86. [PubMed: 17116468]

32. Ceroni A, Maass K, Geyer H, Geyer R, Dell A, Haslam SM. GlycoWorkbench: a tool for the computer-assisted annotation of mass spectra of glycans. J Proteome Res. 2008; 7:1650–9. [PubMed: 18311910]

33. Xiao ZH, Goldsmith HL, McIntosh FA, Shankaran H, Neelamegham S. Biomechanics of P-selectin PSGL-1 bonds: Shear threshold and integrin-independent cell adhesion. Biophys J. 2006; 90:2221–34. [PubMed: 16387772]

34. Vestweber D, Blanks JE. Mechanisms that regulate the function of the selectins and their ligands. Physiol Rev. [Review]. 1999; 79:181–213.

35. Babu P, North SJ, Jang-Lee J, Chalabi S, Mackerness K, Stowell SR, et al. Structural characterisation of neutrophil glycans by ultra sensitive mass spectrometric glycomics methodology. Glycoconj J. 2009; 26:975–86. [PubMed: 18587645]

36. Huhn C, Selman MH, Ruhaak LR, Deelder AM, Wuhrer M. IgG glycosylation analysis. Proteomics. 2009; 9:882–913. [PubMed: 19212958]

37. Raju TS, Briggs JB, Borge SM, Jones AJ. Species-specific variation in glycosylation of IgG: evidence for the species-specific sialylation and branch-specific galactosylation and importance for engineering recombinant glycoprotein therapeutics. Glycobiology. 2000; 10:477–86. [PubMed: 10764836]

38. Baumann H, Doyle D. Turnover of plasma membrane glycoproteins and glycolipids of hepatoma tissue culture cells. J Biol Chem. 1978; 253:4408–18. [PubMed: 207700]

39. Zhang Y, Neelamegham S. Estimating the efficiency of cell capture and arrest in flow chambers: study of neutrophil binding via E-selectin and ICAM-1. Biophys J. 2002; 83:1934–52. [PubMed: 12324413]

40. Komarova S, Roth J, Alvarez R, Curiel DT, Pereboeva L. Targeting of mesenchymal stem cells to ovarian tumors via an artificial receptor. J Ovarian Res. 2010; 3:12. [PubMed: 20500878]

41. Somers WS, Tang J, Shaw GD, Camphausen RT. Insights into the molecular basis of leukocyte tethering and rolling revealed by structures of P- and E-selectin bound to SLe(X) and PSGL-1. Cell. 2000; 103:467–79. [PubMed: 11081633]

42. Teo GS, Ankrum JA, Martinelli R, Boetto SE, Simms K, Sciuto TE, et al. Mesenchymal stem cells transmigrate between and directly through tumor necrosis factor-alpha-activated endothelial cells via both leukocyte-like and novel mechanisms. Stem Cells. 2012; 30:2472–86. [PubMed: 22887987]

43. Chamberlain G, Smith H, Rainger GE, Middleton J. Mesenchymal stem cells exhibit firm adhesion, crawling, spreading and transmigration across aortic endothelial cells: effects of chemokines and shear. PLoS One. 2011; 6:e25663. [PubMed: 21980522]

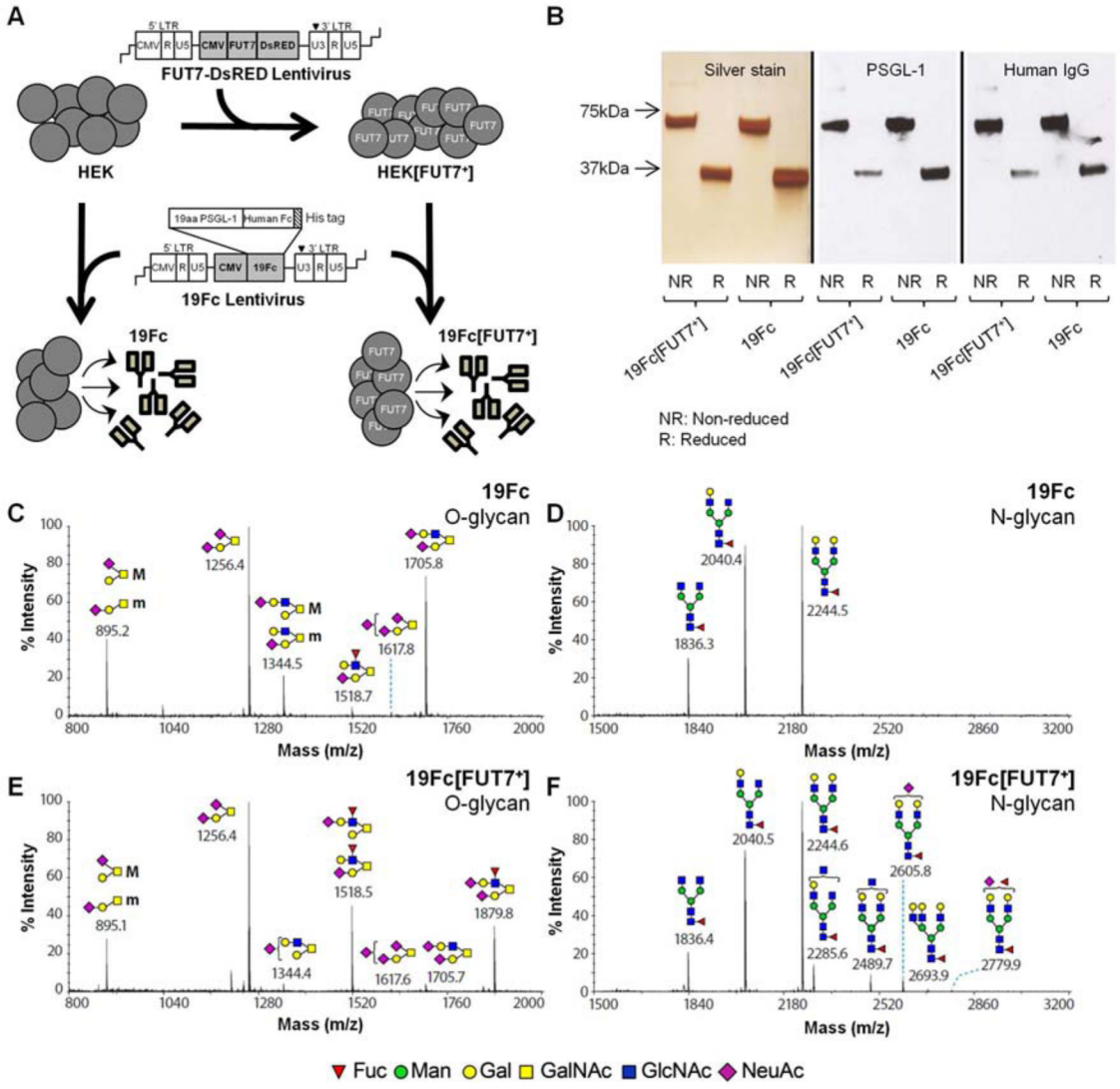


**Fig. 1. Preparation of 19Fc and its variants**

**A.** HEK[FUT7$^+$] cells were generated by transduction of HEK cells with lentivirus encoding for FUT7-DsRED fusion protein. HEK and HEK[FUT7$^+$] cells were transduced with lentivirus to express soluble a His-tagged protein called 19Fc and 19Fc[FUT7$^+$], respectively. **B.** 19Fc or 19Fc[FUT7$^+$] purified from cell culture supernatant using Ni-chelate chromatography was a 68 kDa dimeric protein as shown under non-reducing ('NR') and reducing ('R') conditions. Silver stain shows purity of 19Fc and 19Fc[FUT7$^+$]. Protein identity was verified by performing western blots with anti-PSGL-1 mAb (KPL1) and anti-human IgG Ab. **C.-F.** Glycomics analysis of O-glycans from 19Fc (panel **C**), N-glycans of 19Fc (panel **D**), O-glycans from 19Fc[FUT7$^+$] (panel **E**) and N-glycans of 19Fc[FUT7$^+$] (panel **F**). SLe$^X$ structures at *m/z*=1879.8 and 1518.5 prominently appear in O-glycans of 19Fc[FUT7$^+$] (compare **C** to **E**). Glycan structures in panels C-F are represented using the Consortium of Functional Glycomics nomenclature.

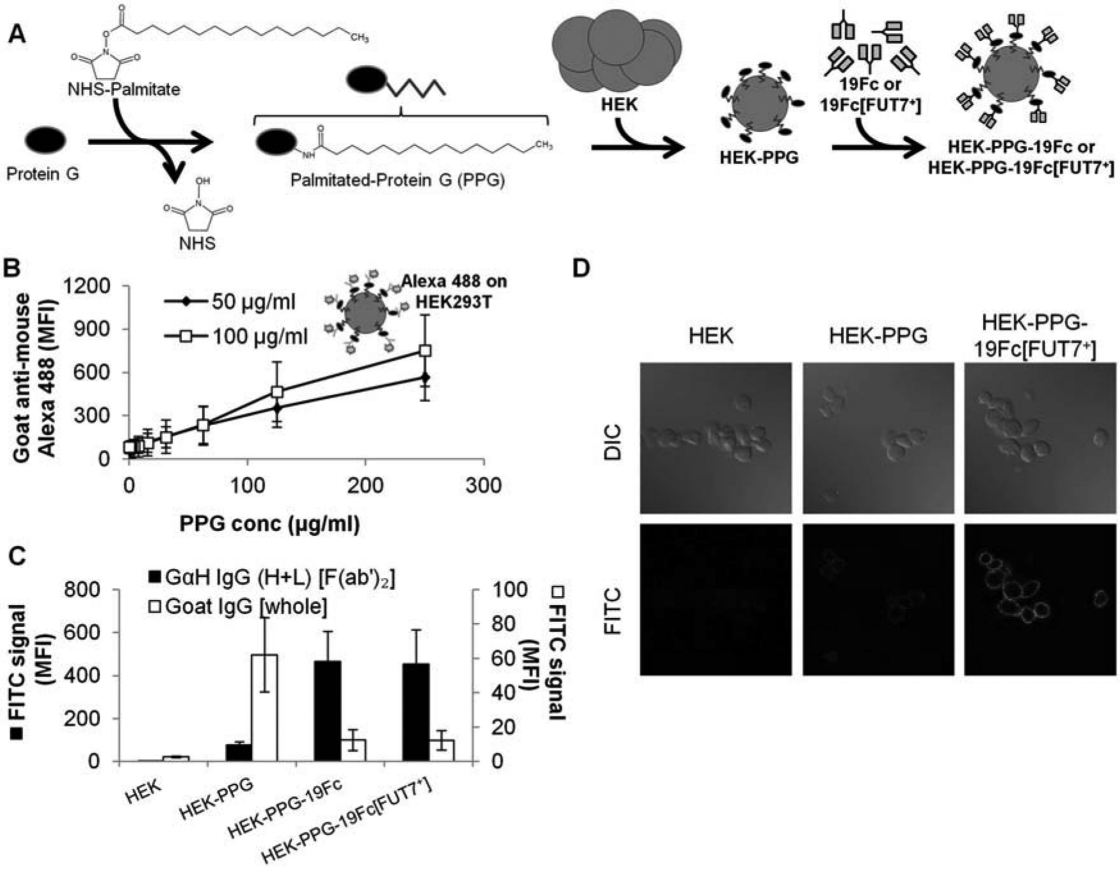


**Fig. 2. Immobilization of 19Fc/19Fc[FUT7$^+$] on HEK cells**

**A.** Palmitated protein G (PPG) was synthesized by reacting NHS-palmitate with protein G. Incubation of PPG with HEK cells lead to its incorporation into the cell membrane. 19Fc or 19Fc[FUT7$^+$] were captured onto cells bearing PPG. **B.** HEK cells with varying concentrations of PPG were incubated with either 50 or 100 μg/ml Alexa 488 conjugated goat anti-mouse IgG [whole antibody]. Antibody immobilization increased with PPG concentration. Data are mean ± SD for three independent experiments. **C.** 50 μg/mL 19Fc or 19Fc[FUT7$^+$] was immobilized on PPG bearing HEK cells. The binding of FITC-conjugated goat anti-human IgG (H+L) [F(ab')$_2$ fragment] (abbreviated GαH IgG (H+L) [F(ab')$_2$], black bar) was enhanced only in the presence of either 19Fc or 19Fc[FUT7$^+$]. On the other hand, the binding of FITC-conjugated goat IgG [whole antibody] (abbreviated Goat IgG [whole], white bar), decreased in the presence of either 19Fc or 19Fc[FUT7$^+$]. Thus, most of the PPG sites were occupied by 19Fc/19Fc[FUT7$^+$]. Data are mean ± SD for four independent experiments. **D.** The binding of FITC conjugated GαH IgG (H+L) [F(ab')$_2$] to HEK-PPG-19Fc[FUT7$^+$] cells in suspension shown using confocal microscopy. Results demonstrate cell-surface localization of 19Fc[FUT7$^+$] on PPG bearing HEK cells. MFI = mean fluorescence intensity.

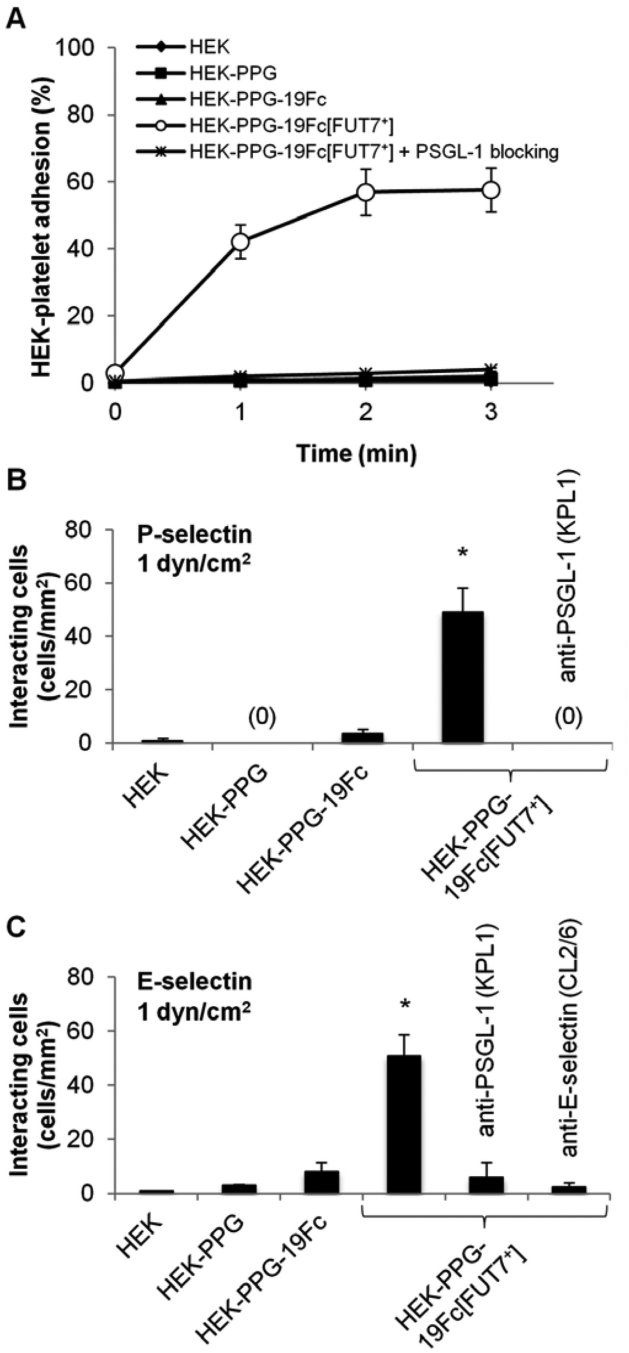


**Fig. 3. HEK cells with immobilized 19Fc[FUT7$^+$] bind E-/P-selectin under shear flow**

**A.** HEK cells bearing 19Fc/19Fc[FUT7$^+$] at 2×10$^6$/mL were mixed with 10$^7$/mL TRAP-6 activated platelets at 650/s in a cone-plate viscometer. % of HEK cells with bound platelets were quantified. 19Fc[FUT7$^+$] but not 19Fc bearing cells bound platelets. Cell adhesion was blocked by anti-PSGL-1 mAb KPL1. Data are mean ± SD for four independent experiments. **B-C.** 2×10$^6$ HEK cells/mL were perfused over either P-selectin bearing CHO-P cells (panel **B**) or E-selectin bearing stimulated HUVECs (panel **C**) at 1 dyn/cm$^2$ in a microfluidic flow chamber. The number of interacting cells was quantified. 19Fc[FUT7$^+$] but not 19Fc bearing cells bound P-/E-selectin bearing substrates. Cell adhesion was blocked by anti-PSGL-1

mAb KPL1 and anti-E-selectin mAb CL2/6. Data are mean ± SD for three independent experiments. * indicates $P < 0.001$ with respect to all other conditions.

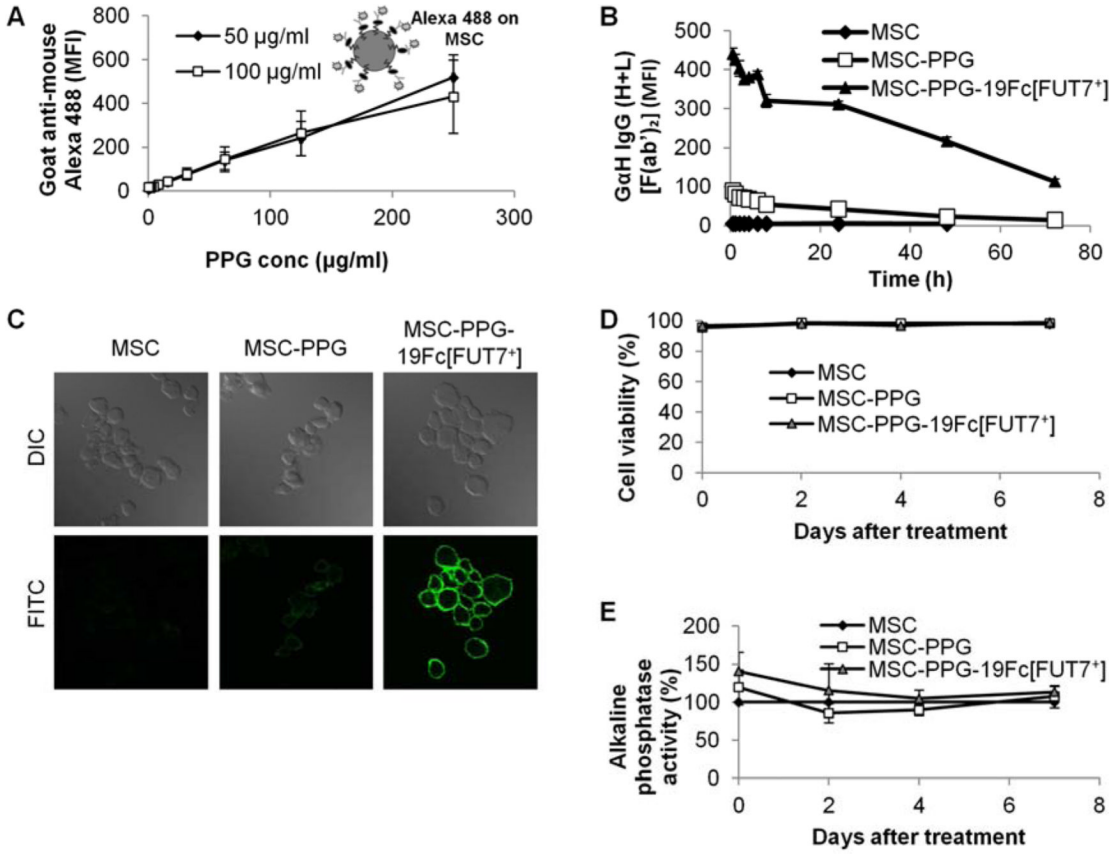


**Fig. 4. 19Fc/19Fc[FUT7$^+$] immobilization on MSCs**

**A.** MSCs were incubated with varied concentrations of PPG. Alexa 488 conjugated goat anti-mouse antibody [whole antibody] measured PPG modification similar to Fig. 2B. Data are mean ± SD for three independent experiments. **B.** FITC conjugated goat anti-human IgG (H+L) [F(ab')$_2$ fragment] monitored the loss of 19Fc[FUT7$^+$] from MSC cell surface over 72 h. (Data are mean ± SD for three independent experiments. Error bars are too small to be visible.) **C.** Confocal microscopy demonstrating cell surface localization of 19Fc[FUT7$^+$] on MSCs similar to Fig. 2D. **D.** Coupling of 100 μg/mL PPG and 100 μg/mL 19Fc[FUT7$^+$] to MSCs did not affect cell viability as measured by trypan blue exclusion. (Data are mean ± SD for three independent experiments. Error bars are too small to be visible.) **E.** The cell coupling procedure did not significantly affect cellular alkaline phosphatase activity. Data are mean ± SD for three independent experiments.

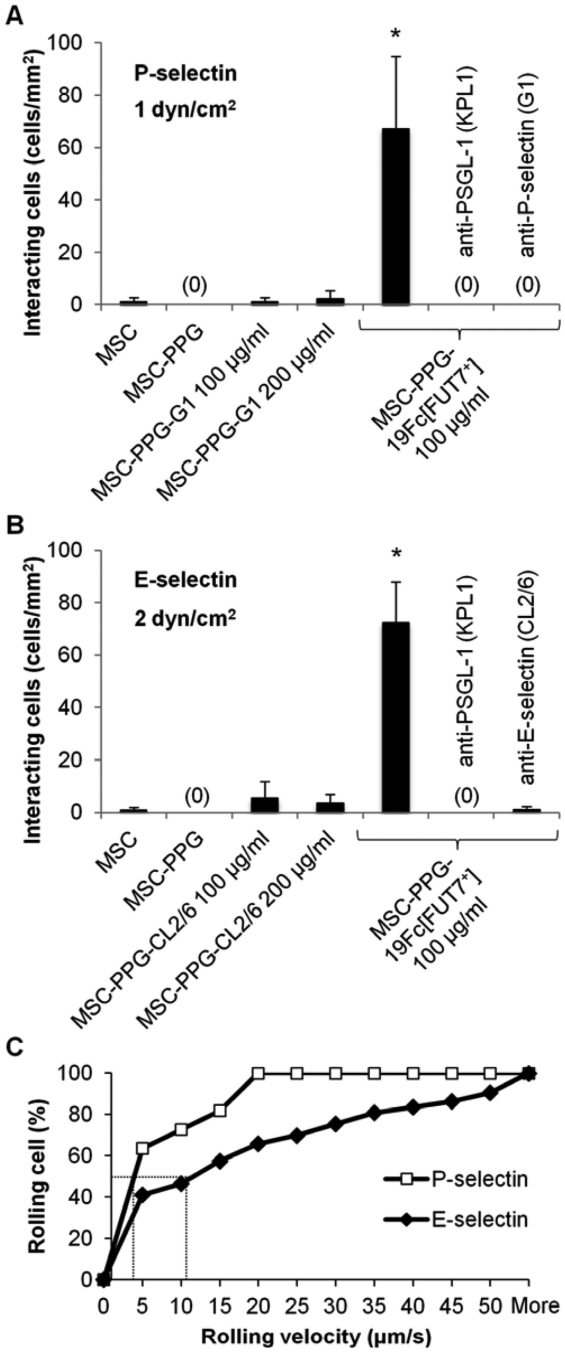


**Fig. 5. MSC-PPG-19Fc[FUT7$^+$] binding to P- and E-selectin in microfluidic flow chamber**

**A-B.** 2-5×10$^6$ MSCs/mL immobilized with either 100 μg/mL 19Fc[FUT7$^+$], 100-200 μg/mL anti-P-selectin mAb G1 or 100-200 μg/mL anti-E-selectin mAb CL2/6 were perfused over either P-selectin bearing CHO-P cells at a wall shear stress of 1 dyn/cm$^2$ (panel **A**) or E-selectin bearing stimulated HUVECs at 2 dyn/cm$^2$ (panel **B**). Only the MSC-PPG-19Fc[FUT7$^+$] cells bound the selectin bearing substrate. Cell interaction was specifically blocked using anti-PSGL-1 mAb KPL1, anti-P-selectin mAb G1 or anti-E-selectin mAb CL2/6 as indicated. Data are mean ± SD for 3-4 independent experiments. * indicates P < 0.001 with respect to all other conditions. **C**. Cumulative rolling velocity plot

showing median rolling velocity of 3 μm/s when MSC-PPG-19Fc[FUT7$^+$] roll on P-selectin/ CHO-P cells at 1 dyn/cm$^2$ and 11.5 μm/s for rolling on E-selectin/ HUVECs at 2 dyn/cm$^2$. The rolling characteristics of 190 cells were analyzed and binned from three independent runs.

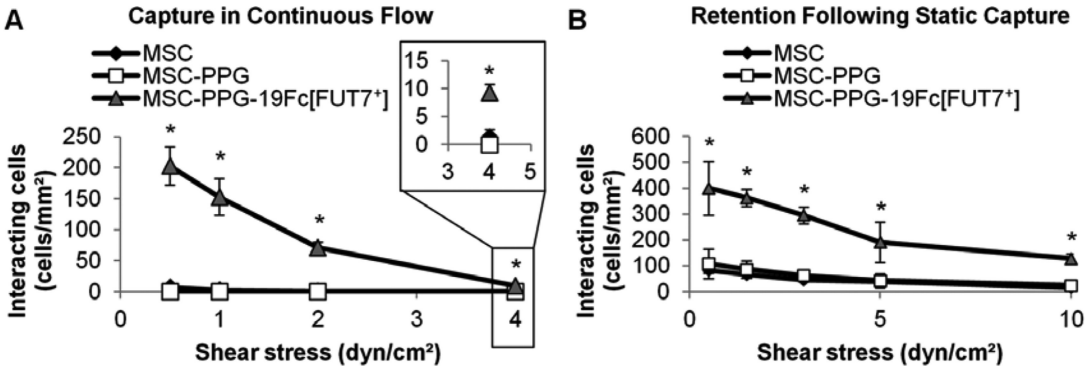


**Fig. 6. Capture and retention of MSC-PPG-19Fc[FUT7$^+$]s on stimulated HUVECs upon varying wall shear stress**

**A.** $5\times10^6$ MSCs/mL were perfused over stimulated HUVECs at various wall shear stresses. Greater number of MSC-PPG-19Fc[FUT7$^+$] cells captured/tethered onto HUVECs compared to either unmodified MSCs or MSC-PPG cells up to 4 dyn/cm$^2$. Data are mean ± SD for three independent experiments. **B.** $5\times10^6$ MSCs/mL were incubated with stimulated HUVEC monolayers under static conditions for 10 min. The applied wall shear stress was then step increased in 3 min intervals at each shear stress until a final wall shear stress of 10 dyn/cm$^2$ was achieved between 12-15 min. MSC-PPG-19Fc[FUT7$^+$] cells, but not other cell types, were robustly retained at all shear stresses. Data are mean ± SD for four independent experiments. * $P < 0.01$ with respect to MSC or MSC-PPG cells.